Jour. of the KGS Vol. 17, No. 3. June 2001, pp 69~75

Effect of Underground Cavity on Bearing Capacity of Strip Footing

지하공동 위에 설치된 기초의 지지력

Jun, Jin-Taek*1 전 진 택
Kim, Young-Uk*2 김 영 욱

요 지

본 논문에서는 지하공동 위에 설치된 띠 기초의 지지력에 대하여 upper bound theory를 이용하여 연구하였다. 기초 크기, 공동의 크기 및 위치, 그리고 지반의 물성치의 영향에 관하여 고찰하였으며 10개의 파괴 형상에 대하여 분석을 수행하였다. 각각의 파괴형상은 지반의 물성치 및 기하학적인 형상에 관한 함수로 표현되어 컴퓨터 해석을 통한 최소화를 시행하였다. 최소화를 위한 프로그램은 Boland C++ Builder를 이용하여 작성한 후 PC에서 수행되었다. 10개의 파괴형상 중 최소의 기초 지지력을 작성된 컴퓨터 프로그램을 통하여 구하였고 이를 해당 기초의 극한 지지력으로 추정하였다. 본 연구의 결과를 종합 정리하여 지하공동 위에 위치한 띠 기초의 극한 지지력을 구할 수 있는 간단한 식을 제시하였다.

Abstract

Using the upper bound theorem of limit analysis, the effect of continuous circular cavities on the collapse load of overlying strip surface footings was investigated. The analysis was undertaken for a range of footing size, cavity size, and soil property through ten collapse mechanisms. For each collapse mechanism, a collapse footing pressure equation was developed as a function of soil property and the geometry of the mechanism. Then, the collapse footing pressure of each mechanism was minimized with respect to the parameters that describe the geometry. The minimization was performed on a PC using a computer program written in Boland C^{++} Builder language for a Windows 95 or NT. The smallest collapse footing pressure obtained from the ten collapse mechanisms was taken as the ultimate bearing capacity of the footing. Based on the results of analysis, correlation equations and figures were developed in the study. These equations and figures can be used to determine the influence zone, the critical depth to cavity, and the ultimate bearing capacity of a strip footing underlain by a cavity.

Keywords : Collapse load, Collapse mechanism, Critical depth, Influence zone, Limit analysis, Strip footing, Ultimate bearing capacity, Underground cavity/void, Upper bound theorem

1. Introduction

Underground cavities can be either naturally formed, e.g. solution cavities in soluble rocks, or man-made, e.g. tunnels or mine cavities. When cavities are near footings, they may interact with each other resulting in adverse effect of the cavity on the footing performance. Numerous studies related to this subject matter are available; some of the studies deal with cavity-footing interaction, e.g. Badie and Wang(1994), Wood and

*1 Engineer, Patel Chen Associates, Inc., U.S.A.
*2 Member, Assistant Professor, Dept. of Civil & Environmental Engrg., Myongji Univ.

Larnach(1985), Badie and Wang(1984,1985), and Abdellah and Abdalla(1987). There are also studies concerning the determination of bearing capacity of footings above cavities, e.g. Wang and Hsieh(1987). All of these studies provide fundamental bases for the development of a generally accepted methodology for analysis and design of footings underlain by cavities.

An essential element in the design methodology is the method for determination of bearing capacity under varying conditions of cavity, footing, loading, and soil property. The available methods for the determination of bearing capacity are developed only for limited cavity and soil conditions. To develop a method that can consider a broader range of conditions, a study was undertaken using the upper bound theorem of limit analysis. The result of the study including ultimate bearing capacity as well as charts which delineate influence zones and contours of equal percentage of bearing capacity are presented herein.

2. Formulation

The analysis is made using the upper bound theorem of limit analysis for strip footings overlying and parallel with continuous circular cavities. The footing having a

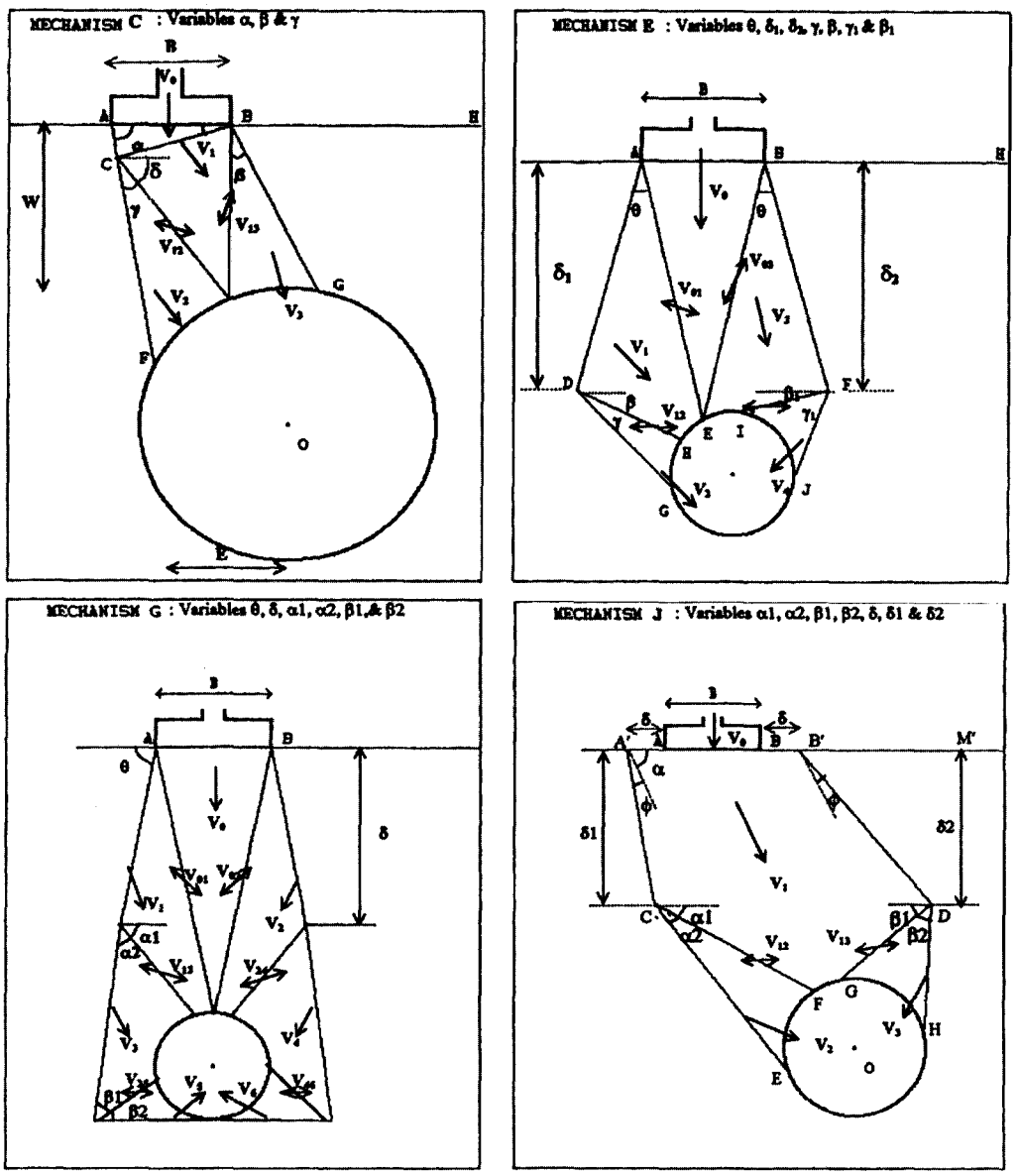

Fig. 1 Collapse mechanisms C, E, G, and J

width of B is rigid and is subjected to a vertical central load. The circular cavity having a diameter of W is located at a depth of D (vertical distance between footing base and cavity top) with an eccentricity of E (horizontal distance between footing and cavity centers). The supporting soil behaves as a rigid-plastic material that can be characterized by c(cohesion) and $\varnothing$ (internal friction angle).

In the analysis of collapse footing pressure, ten collapse mechanisms (mechanism A through J) were considered. These mechanisms were conjectured based on the available information on the failure surfaces observed from the finite element analysis and the model footing tests of Baus(1980), Badie(1983), and others. Four (mechanisms C, E, G, and J) of the ten collapse mechanisms are illustrated in Fig. 1; these four me- chanisms, under most conditions, provide smaller collapse footing pressures than the other mechanisms. For each collapse mechanism, the rate of energy dissipation along the slip lines and the rate of work done by footing pressure, soil weight, and fluid pressure inside the cavity, if any, were obtained. By equating the rate of energy dissipated and rate of work done, the equation for collapse footing pressure as a function of footing size, cavity size and location, and soil property was formulated. Each equation contained one or more variables that define the geometry of the collapse mechanism.

Presented below are the footing pressure equations formulated for mechanism J.

Note that, in the equations, the pressure inside the cavity is assumed to be the atmospheric pressure. Also, the external work done by the soil weight is expressed in terms of area rather than volume of the soil mass involved, since the two-dimensional analysis made for a unit footing length. It is seen that the equations are complex and very lengthy. Therefore, equations are presented only for one of the ten mechanisms analyzed.

Mechanism J

$$q_0 = \frac{1}{B}\Big[c \cdot \cos\varnothing \cdot \Big\{\frac{L_{AC}+L_{B'D}}{\sin\alpha} + L_{CE}\cdot\omega_2 + L_{DH}\cdot\omega_3 + L_{CF}\cdot\omega_{12} + L_{DG}\cdot\omega_{13}\Big\} - \gamma\cdot\{A_{A'CFGDB'} + A_{CEF}\cdot\omega_2\cdot\sin(\alpha_1+\alpha_2-\varnothing) + A_{DGH}\cdot\omega_3\cdot\sin(\beta_1+bet_2-\varnothing)\}\Big] \quad (1)$$

with $\omega_2 = \dfrac{\sin(\alpha_1+\alpha_2-\varnothing)}{\sin\alpha\cdot\sin(2\alpha_1+\alpha_2-2\varnothing)}$, and

$\omega_{12} = \dfrac{\sin(\alpha-\alpha_1-\alpha_2+\varnothing)}{\sin\alpha\cdot\sin(2\alpha_1+\alpha_2-2\varnothing)}$ for $\alpha_1 < \varnothing$

$\omega_2 = \dfrac{\sin(\alpha_1+\alpha_2-\varnothing)}{\sin\alpha\cdot\sin\alpha_2}$, and

$\omega_{12} = \dfrac{\sin(\alpha-\alpha_1-\alpha_2+\varnothing)}{\sin\alpha\cdot\sin\alpha_2}$, for $\alpha_1 > \varnothing$

$\omega_3 = \dfrac{\sin(\alpha+\beta_1-\pi-\varnothing)}{\sin\alpha\cdot\sin\beta_2}$, and

$\omega_{13} = \dfrac{\sin(\beta_1+\beta_2+\alpha-\varnothing)}{\sin\alpha\cdot\sin\beta_2}$ for $\beta_1 < \varnothing$

$\omega_3 = \dfrac{\sin(\beta_1-\alpha-\varnothing)}{\sin\alpha\cdot\sin\beta_2}$, and

$\omega_1 = \dfrac{\sin(\beta_1+\beta+\alpha_2-\varnothing)}{\sin\alpha\cdot\sin\beta_2}$ for $\beta_1 > \varnothing$

in which q_0 = collapse footing pressure

$L_{withscripts}$ = length of line segment identified by subscripts

$A_{withscripts}$ = area of soil mass identified by subscripts

B = footing width

c = cohesion of soil

$\varnothing$ = internal friction angle of soil

γ = unit weight of soil

$\alpha_1, \alpha_2, \beta_1, \beta_2, \delta_1, \delta_1$, and δ_2 = variables to be optimized

3. Computer Analysis

To obtain the collapse footing pressure, the footing pressure in each equation needs to be minimized with respect to the variables. Because of the complexity of the equations, it is very difficult, if not impossible, to present the minimized equation in a simple form. Therefore, the minimization was performed on a PC Pentium 133 with an 8Mbytes RAM. The computer program was written in Boland C++ Builder language for Windows 95 or NT. In addition to the computer analysis for footings above cavities, the collapse footing pressures of footings without cavities (no-cavity condition) were also computed from Hill's mechanism (Chen, 1974).

4. Result and Analysis

The collapse footing pressures for footings above cavities are expressed as a percentage of no-cavity condition, and are related with D/B for different W/B and E/B values. Fig. 2 presents the relationship between collapse footing pressure and D/B for W/B=3.0 and E/B=1.0. Also included in the figure is the collapse footing pressure obtained for soil properties of γ=103.7 pcf(16.5 kN/m^3), c=3,312 psf (158.6 kN/m^2), and $\varnothing$= 8°. These are the soil properties used in the previous studies. There are more graphical relations for different vales of W/B and E/B with different soil properties which are not presented. Fig. 2 indicates that for the soil and cavity conditions analyzed, mechanism J is most critical.

The lowest value of collapse footing pressure determined

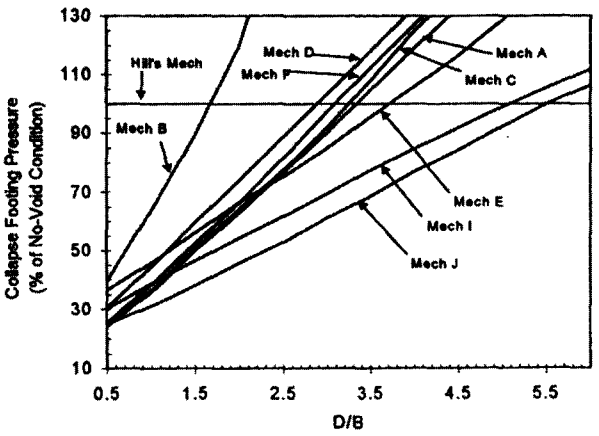

Fig. 2 Collapse footing pressure vs. D/B for W/B=3 and E/B=1

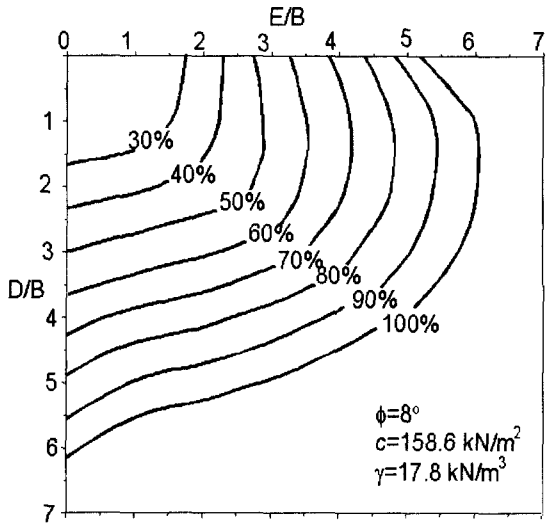

Fig. 3 Contours of equal percentage of no-cavity ultimate bearing capacity for W/B=3.0

from the various collapse mechanisms can be taken as the ultimate bearing capacity of the footing. As would be expected, Fig. 2 shows that the ultimate bearing capacity increases with increasing D/B to 100% at D/B $\approx$5.5. The depth at this D/B ratio of 5.5 is termed the critical depth (Baus and Wang, 1983), since below this depth, the ultimate bearing capacity remains at 100% indicating no effect of cavity on footing stability. When the cavity is located above the critical depth the footing stability will be adversely influenced by the cavity. Thus, the zone between footing base and critical depth can be termed as the influence zone.

From the graphs which relate the ultimate bearing capacity and D/B, the influence zone for different W/B can be generated. In addition, within the influence zone, contours of equal percentage of no-cavity ultimate bearing capacity can be obtained. Fig. 3 presents such a graph for W/B=3.0 with c=3,312 psf(158.6 kN/m^2), $\varnothing$=8°, and γ=103.7 pcf(17.8 kN/m^3).

The influence zone graphs are further modified to take into account the soil property. The modified graphs are shown in Figs. 4(A), (B), and (C) for 100%, 75%, and 50% of no-cavity ultimate bearing capacity, respectively. In these figsures, the parameters η and λ are defined as follows:

$$\eta = \frac{D}{W} \cdot \left(\frac{1+W/B}{2} - \frac{W/B}{10}\right) \cdot \left(\frac{50}{\varnothing + 50}\right) \cdot \lambda \qquad (2)$$

$$\lambda = \frac{c}{\gamma \cdot B} \qquad (3)$$

Note that when applied to 100% of no-cavity ultimate bearing capacity contours in Fig. 4(A), the term D becomes D_{cr}. It is seen that η is a function of not only the depth to cavity but also the cavity size and soil property. The soil property is also considered in λ. The range of soil property analyzed is c=500 to 3,000 psf (23.9 to 143.6 kN/m^2), $\varnothing$=5° to 35°, and γ=100 to 130 pcf (15.7 to 20.4 kN/m^3). Both Figs. 4(B) and (C) contain two zones; the zone with solid lines is valid for all values of W/B analyzed, while the zone with dashed lines is valid only for W/B greater than a certain value. These three Figs. can be used to estimate the ultimate bearing

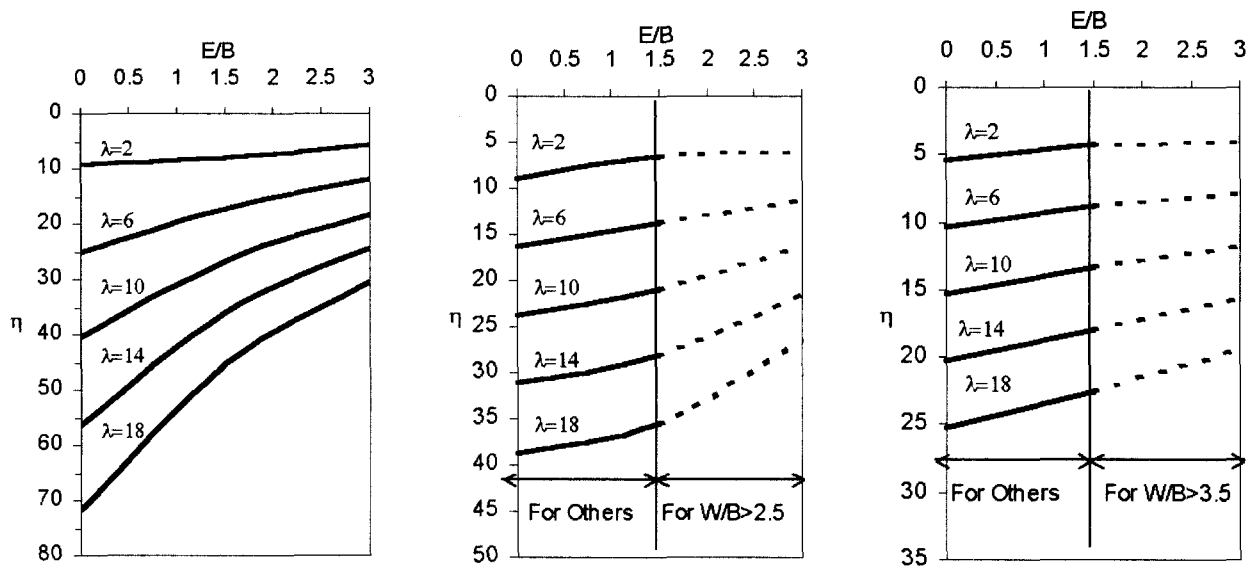

(a) Contours of 100% no-void ultimate bearing capacity

(b) Contours of 75% no-void ultimate bearing capacity

(c) Contours of 50% no-void ultimate bearing capacity

Fig. 4

capacity for a given cavity size, cavity location, and soil property.

The critical depth data presented in Fig. 4(A) and others which have been computed but not presented, are further integrated in Fig. 5. Fig. 5 relates parameters η with λ for a constant E/B; three values of E/B, i.e. 0, 1.5, and 3.0, are presented. Along each graphical relation are shown data points obtained for different internal friction angles of 5°, 15°, and 35°. The data points fluctuate along the line in a narrow range without a definite pattern, suggesting that the internal friction angle has little effect on the correlation. The regression analysis of the data shows the following relations:

$$\eta = 1.5988 + 3.9131\lambda \quad \text{for} \quad E/B = 0 \tag{4}$$

$$\eta = 3.3085 + 2.3513\lambda \quad \text{for} \quad E/B = 1.5 \tag{5}$$

$$\eta = 2.6838 + 1.5593\lambda \quad \text{for} \quad E/B = 3.0 \tag{6}$$

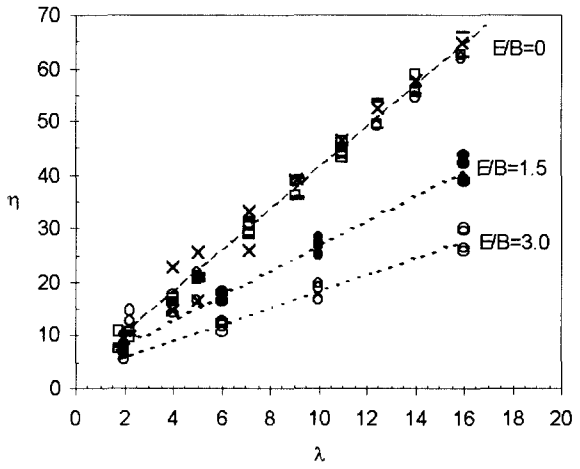

Fig. 5 Relation between η and γ for E/B=0, 1.5, and 3.0

For the correlation, the adjusted R-square values are 0.986, 0.985 and the p-values are 0.0052, 0.00055 and 0.0043 for E/B=0, 1.5, and 3.0, respectively. These regression parameters indicate a very good fit of the equations to the data points.

Equations (4), (5), and (6) were developed from 100% of no-cavity ultimate bearing capacity data. Therefore, in the η definition, i.e. Equation (2), the depth to void (D) should be replaced by critical depth (D_{cr}). From these equations, i.e. Equations (2) through (6), the critical depth void can be determined for a given soil property and void size.

5. Discussions

To determine the critical depth using Equations (4), (5), or (6), the value of parameter λ must be computed first. The value of λ is entered in Equations (4), (5), or (6) to find η. Then, D_{cr} is computed for the given values of W, B, and $\varnothing$ using Equation (2). When E/B value

is different from 0, 1.5, and 3.0, the method of interpolations is needed. The following example illustrates the procedures.

A 3-ft (0.91-m) wide strip footing overlies a 2-ft (0.61-m) diameter circular cavity which is 3-ft (0.91-m) off the footing center. The foundation soils has c=1,200 psf (57.5kN/m^2), $\varnothing$=15°, and γ=120 pcf (18.9 kN/m^3). From these soil properties and footing size, $\lambda = c/\gamma B$ =3.33 and kN/m^2. Using Equations (4), (5), and (6), the computed η values are η =14.63 for E/B=0, η=11.14 for E/B=1.5, and η =7.88 for E/B=0.67 and λ=3.33 into Fig. 4(A), the value of η is about 12.5. Then, from Equation (2), the computed D_{cr} equals 16.0 ft(14.9m).

The critical depth data thus obtained are plotted against the available data of Baus and Wang(1987), Badie and Wang(1985), and Hsieh and Wang(1987) in Fig. 6. Also included in the figure is a 45°-line. Note that the available data were obtained from the results of finite element analysis which characterized the foundation soil as an elasto-plastic material. The upper bound theorem of limit analysis adopted in this study characterized the soil as rigid-plastic material as stated earlier.

The data presented in Fig. 6 are generated from three soils - a kaolin (c=158.5 kN/m^2 and $\varnothing$=8°), a silty clay (c=65.5 kN/m^2 and $\varnothing$=13.5°) and clayey sand(c=9.2KN/m^2 and $\varnothing$=31.0°). This Fig. shows that, except for four data points - two dotted triangles and two dotted circles,

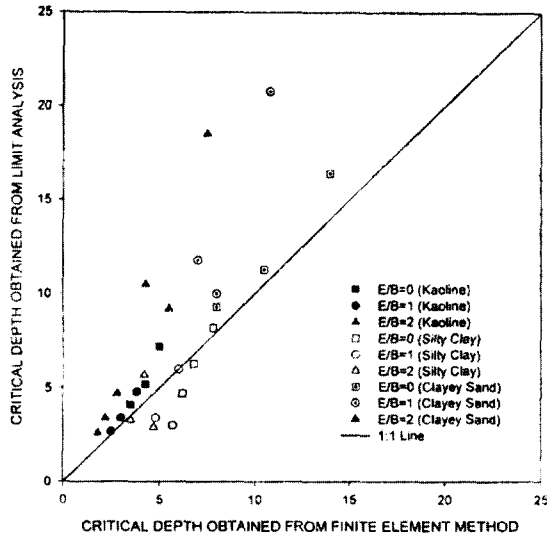

Fig. 6 Critical depth obtained from limit analysis vs. FEM

which are far away from the 45° - line, the agreement between the two sets of data, generally speaking, is fairly good. These four outliers are obtained from the clayey sand. It is also seen that all of the data points of the clayey sand are located above the 45° - line. This may suggest that the clayey sand may not be best characterized as a rigid-plastic material in the limit analysis.

While Fig. 3 represents the critical depth contour (100% curve), it also contains contours of equal percentage of no-cavity ultimate bearing capacity for a given soil property with W/B=3.0. For other void sizes, void location, and soil properties, the ultimate bearing capacity can be estimated from Figs. 4(A), 4(B), and 4(C), as mentioned earlier. The previous example is extended here to demonstrate its applications. For the 2-ft(0.61m) diameter cavity located at E/B=1.0 and D/B=3.0, the ultimate bearing capacity of the overlying 3-ft(0.91-m) wide strip footing is estimated as below.

First, calculate parameter λ, which is equal to 3.33. From Equation (2), compute η which equals 8.85. Enter E/B=1.0 and λ=3.33 in Figs. 4(A), 4(B), and 4(C), and get $\eta \approx$ 12.5, 10.0 and 6.1, respectively. These η values of 12.5, 10.0, and 6.1 are corresponding to 100%, 75% and 50% of no cavity ultimate bearing capacity, respectively. By graphical interpolation, the percentage of bearing capacity corresponding to η=8.85 is approximately 67% of no-cavity ultimate bearing capacity.

According to Hill's mechanism, the no-cavity ultimate bearing capacity equals 13,363 psf(640 kN/m^2). Thus, the ultimate bearing capacity of the footing in question equals approximately 8,953 psf(429 kN/m^2).

The aforementioned examples have demonstrated the potential usage of the developed equations and figures for stability analysis of strip footings overlying circular cavities. In applications, it should be reminded of the conditions from which the equations and figures were developed. The conditions include vertical central loading on strip surface footing underlain by a continuous circular cavity together with the range of cavity size, cavity locations, and soil properties stated earlier. While application may require interpolation within the range of conditions investigated, extrapolation beyond the range should be made with caution.

6. Summary and Conclusions

The stability of strip footing overlying a continuous circular cavity was investigated using the upper bound theorem of limit analysis. The collapse footing pressure under vertical central loading was analyzed for a range of cavity size (W/B=0.5 to 3.0), cavity location (D/B =0.5 to 7.5, E/B=0 to 6.0) and soil properties(c=500 to 3,000psf, $\varnothing$=5° to 35°, γ=100 to 130 pcf). From the results of analysis, correlation equations and charts were developed for determination of critical depth to void as well as the ultimate bearing capacity of the footing. Examples were given to demonstrate that the results of analysis using the upper bound theorem of limit analysis have provided a database useful for stability analysis of strip footing overlying continuous circular cavities.

References

1. Abdellah, G. A. H. and Abdalla, M. H. (1987), "The Interaction Between a Tunnel/Cavity and Nearby Structures," Proc. VI Australian Tunneling Conference, Vol. 1, pp. 183-189.
2. Badie, A. (1983), "Stability of Spread Footing Supported by Clay Soil with Underground Void," Ph. D thesis, The Pennsylvania State University, University Park, PA.
3. Badie, A. and Wang, M. C. (1984), "Stability of Spread Footing Above Void in Clay," J. Geotech. Engrg. Div., ASCE, Vol. 110, No. 11, pp. 1591-1605.
4. Badie, A. and Wang, M. C. (1994), "Interaction Between Strip Footing and Soft Ground Tunnel," Proc., XIII International Conference on Soil Mechanics and Foundation Engrg., New Delhi, India, Vol. 2, pp. 571-574.
5. Baus, R. L. (1980), "The Stability of Shallow Continuous Footings Located above Voids," Ph. D thesis, The Pennsylvania State University, University Park, PA.
6. Baus, R. L. and Wang, M. C. (1983), "The Bearing Capacity of Strip Footing Located above a Void in Cohesive Soils," J. Geotech. Engrg. Div., ASCE, Vol. 109, No. 1, pp. 1-14.
7. Chen, W. F. (1974), Limit Analysis and Soil Plasticity, Elsevier Scientific Co., New York, NY.
8. Hsieh, C. W. and Wang, M. C. (1992), "Bearing Capacity Determination Method for Strip Surface Footings Underlain by Voids," Transportation Research Record No. 1336, Transportation Research Board, pp. 90-95.
9. Wang, M. C. and Badie, A. (1985), "Effect of Underground Void on Foundation Stability," J. Geotech. Engrg., ASCE, Vol. 111, No. 8, pp. 1008-1019.
10. Wang, M. C. and Hsieh, C. W. (1987), "Collapse Load of Strip Footing above Circular Void," J. Geotech. Engrg., ASCE, Vol. 113, No. 5, pp. 511-515.
11. Wood, L. A. and Larnach, W. J. (1985), "The Behavior of Footings Located above Voids," Proc. Eleventh International Conference on Soil Mechanics and Foundation Engrg., San Francisco, CA. pp. 2273-2276.

(received on May 4, 2001)